

# Supporting Information

## Receptor and Microenvironment Dual-Recognizable Nanogel for Targeted Chemotherapy of Highly Metastatic Malignancy

*Jinjin Chen,<sup>†,§,⊥</sup> Jianxun Ding,<sup>†,⊥</sup> Weiguo Xu,<sup>†</sup> Tianmeng Sun,<sup>‡</sup> Haihua Xiao,<sup>†</sup> Xiuli Zhuang,<sup>†</sup> and Xuesi Chen<sup>\*†</sup>*

<sup>†</sup>Key Laboratory of Polymer Ecomaterials, Changchun Institute of Applied Chemistry, Chinese Academy of Sciences, Changchun 130022, People's Republic of China

<sup>‡</sup>The First Hospital and Institute of Immunology, Jilin University, Changchun 130061, People's Republic of China

<sup>§</sup>University of Chinese Academy of Sciences, Beijing 100039, People's Republic of China

### Author Contributions

<sup>⊥</sup>J. Chen and J. Ding contributed equally to this work.

### Corresponding Authors

\*E-mail: xschen@ciac.ac.cn (X. Chen).

## MATERIALS AND METHODS

**Materials.** Methoxy tri(ethylene glycol) (mTEG) was purchased from Aladdin Industrial Co. (Shanghai, P. R. China). L-Glutamic acid, L-phenylalanine (LP), and L-cystine (LC) were obtained from GL Biochem, Ltd. (Shanghai, P. R. China). mTEGLG NCA, LP NCA, and LC NCA were prepared in the same pathway as reported in previous works.<sup>1,2</sup> *N,N*-Dimethylformamide (DMF) was pretreated with calcium hydride (CaH<sub>2</sub>) and then purified by vacuum distillation at 45 °C. 4-(Aminomethyl)phenylboronic acid hydrochloride and 4-(2-aminopropyl)morpholine were purchased from Tokyo Chemical Industry (TCI, Tokyo, Japan) and used without further purification. Doxorubicin hydrochloride (DOX·HCl) was obtained from Beijing Huafeng United Technology Co., Ltd. (Beijing, P. R. China).

**Syntheses and Characterizations of PNG and PMNG.** Firstly, 13.0 mg of 4-(aminomethyl)phenylboronic acid hydrochloride and 3.9 mg of 4-(2-aminopropyl)morpholine were dissolved in 100.0 mL of DMF. Then, 320.0 mg of mTEGLG NCA was added to the solution and stirred for three days. Finally, 191.0 mg of LP NCA and 146.0 mg of LC NCA were added into the above solution with stirring for another three days. The obtained solution was poured into 500.0 mL of ethyl ether, and the precipitate was collected. After drying of the product *in vacuo*, PMNG was obtained with the yield of 80.4%. PNG was prepared in the similar route as PMNG using 4-(aminomethyl)phenylboronic acid hydrochloride only as an initiator. The products were characterized by proton nuclear magnetic resonance (<sup>1</sup>H NMR), Fourier-transform infrared (FT IR), inductively coupled plasma optical emission spectroscopy (ICP-OES), and elemental analysis.

The morphologies and sizes of PNG and PMNG were measured by both transmission electron microscope (TEM) and dynamic light scattering (DLS). The changes in sizes after incubation with 10.0 mM GSH were also carried out as follows. The nanogels were dissolved in ultrapure water at a concentration of  $0.1 \text{ mg mL}^{-1}$ , and then GSH was added into the solution with the concentration of 10.0 mM. At the time points of 0, 2, 4, and 8 h, the sizes of nanogels were determined by DLS, and a drop of the solution was dropped onto the carbon-coated copper mesh for TEM analysis. The zeta potentials were also detected in various pH values from 6.0 to 7.4 on a zeta potential analyzer (ZETA PALS, Brookhaven instruments corporation, USA).

**Preparations and Characterizations of PNG/DOX and PMNG/DOX.** DOX was chosen as a model drug and loaded into the cores of nanogels through diffusion and dialysis. Typically, 10.0 mg of DOX and 50.0 mg of PMNG were codissolved in 10.0 mL of DMF. And then, 10.0 mL of ultrapure water containing 1.0 mL of phosphate-buffered saline (PBS) was added into the solution. After stirring for 12 h, the solution was moved into a dialysis bag (molecular weight cut-off (MWCO) = 3500 Da) and dialyzed against ultrapure water for 8 h. The water was replaced by fresh one every 2 h. Finally, the solution was lyophilized with deionized water, and PMNG/DOX was obtained. PNG/DOX was prepared according to the similar protocol.

The drug release behaviors of DOX-loaded nanogels were carried out in different conditions, simulating physiological and tumor environments. PMNG/DOX was dissolved in PBS at pH 7.4 or 6.5, or PBS at pH 7.4 containing 10.0 mM GSH, mimicking the intracellular reductive microenvironment. Then, the solution was put into a dialysis bag

(MWCO = 3500 Da) and incubated with 100.0 mL of corresponding buffers. At predetermined time intervals, 2.0 mL of the buffers were collected and another 2.0 mL of fresh buffers were added into the solution to maintain the total volumes. The concentrations of DOX in the collected buffers were then detected by a Photon Technology International Fluorescence Master System with the software Felix 4.1.0 (Lawrenceville, NJ, USA). The drug release behavior of PNG/DOX was also carried out in the same approach.

**Cell Uptakes and Intracellular Payload Release of PNG/DOX and PMNG/DOX.** The cell uptakes and intracellular release behaviors of PNG/DOX and PMNG/DOX were evaluated by flow cytometer (FCM) and confocal laser scanning microscope (CLSM) toward B16F10 cells, that is, a highly metastatic cell line.

**FCM.** The B16F10 cells were seeded in 6-well plates at about  $2.0 \times 10^5$  cells per well in 2.0 mL of complete Dulbecco's modified Eagle's medium (DMEM) containing 10% (*V/V*) fetal bovine serum (FBS), 50.0 IU mL<sup>-1</sup> penicillin, and 50.0 IU mL<sup>-1</sup> streptomycin, and cultured for 24 h. Then, the medium was removed, and free DOX, PNG/DOX, or PMNG/DOX at an equivalent DOX concentration of 10.0 µg mL<sup>-1</sup> in 2.0 mL of complete DMEM at pH 7.4 or 6.5 was added. For the competitive assay, the cells were preincubated with 4.0 mM of free PBA, 10.0 mM of GSH, or 40.0 mU mL<sup>-1</sup> of sialidase for 10 min, 2 h, or overnight before addition of DOX formulations, respectively. The sialidase could accelerate the hydrolysis of terminal SA residues on the cell membrane. The cells were further incubated for another 2 h. Afterwards, the medium was removed, and cells were washed thrice using PBS and treated with trypsin. Subsequently, the cells in each well were suspended in 1.0 mL of PBS and centrifuged at 1000 rpm for 4 min. After removing the

supernatants, the cells were resuspended in 0.3 mL of PBS. Data for 10,000 gated events were collected, and analyses were performed using a FCM (Millipore, Billerica, MA, USA).

**CLSM.** The cells were seeded in 6-well culture plates at around  $2.0 \times 10^5$  cells per well in 2.0 mL of complete DMEM. The culture medium was removed after 24 h of incubation, and free DOX, PNG/DOX, or PMNG/DOX at an equivalent DOX concentration of  $10.0 \mu\text{g mL}^{-1}$  in 2.0 mL of complete DMEM at pH 7.4 or 6.5 was added subsequently. For the competitive assay, the cells were pretreated with 4.0 mM of free PBA, 10.0 mM of GSH, or  $40.0 \text{ mU mL}^{-1}$  of sialidase for 10 min, 2 h, or overnight before the addition of DOX formulations, respectively. After incubation for another 2 h, the culture media were removed. The cells were washed thrice with PBS, fixed with 4% (*W/V*) PBS-buffered formaldehyde for 30 min at 25 °C, and subsequently stained with DAPI for cell nuclei. The CLSM images of cells were obtained on a confocal microscope (ZEISS LSM 780, Carl Zeiss, Jena, Germany).

***In Vitro* Cytotoxicity Assays.** The cytotoxicities of free DOX, PNG/DOX, and PMNG/DOX were analyzed using a (3-(4,5-dimethylthiazolyl-2)-2,5-diphenyltetrazolium bromide) (MTT) assay toward B16F10 cells *in vitro*. The cells were seeded in 96-well culture plates at a density of appropriate 7000 cells per well in 200.0  $\mu\text{L}$  of complete DMEM and incubated for 24 h, followed by removing the culture medium and then adding free DOX, PNG/DOX, or PMNG/DOX ( $0 - 10.0 \mu\text{g mL}^{-1}$  DOX) in 200.0  $\mu\text{L}$  of complete DMEM at pH 7.4 or 6.8. To evaluate the influence of intracellular reduction, the cells were preincubated with 10.0 mM GSH for 2 h before addition of DOX-loaded nanogels. Then, the cells were subjected to MTT assay after incubation for 48 h. The absorbances of above media were

measured at 490 nm on a Bio-Rad 680 microplate reader. The cell viability was calculated based on Equation 1:

$$\text{Cell viability (\%)} = \frac{A_{\text{sample}}}{A_{\text{control}}} \times 100\% \quad (1)$$

In Equation 1,  $A_{\text{sample}}$  and  $A_{\text{control}}$  represented the absorbances of sample and control wells, respectively.

**Cell Migration Assays.** A wound-healing assay was performed to evaluate the impact of DOX-loaded nanogels on cell migration. Cells were firstly plated in 6-well plates and allowed to grow to  $\geq 95\%$  confluent. After washing cells trice with PBS, a sterile pipette tip of 200.0  $\mu\text{L}$  was used to scratch the cell monolayer. Cells were washed again with PBS, photographed to mark original scratched tracks, and then incubated with 2.5 mL of serum-free DMEM containing DOX, PMNG/DOX, or PNG/DOX with an equivalent DOX concentration of 1.0  $\mu\text{g mL}^{-1}$ . After 12 h, the cells were washed with PBS again and photographed to mark the final scratched tracks. The migration rates were analyzed by Equation 2:

$$\text{Migration rate (\%)} = \frac{d_1 - d_2}{d_1} \times 100\% \quad (2)$$

In Equation 2,  $d_1$  and  $d_2$  represented the width of wound at 0 and 12 h, respectively.

**Cell Invasion Assay.** The cell invasion of B16F10 cells was evaluated by a transwell assay as described previously.<sup>3</sup> Transwell chambers (24-well, 8- $\mu\text{m}$  pore size, Costar, Cambridge, MA) were coated with 50.0  $\mu\text{L}$  of DMEM containing 20% ( $V/V$ ) BD Matrigel<sup>®</sup> for 30 min at 37  $^{\circ}\text{C}$ . B16F10 cells were firstly incubated with serum-free DMEM for 12 h and then suspended in 100.0  $\mu\text{L}$  of serum-free DMEM containing different formulations with

an equivalent DOX concentration of  $1.0 \mu\text{g mL}^{-1}$  to a final density of  $1 \times 10^5$  cells per mL. The suspensions were added into the inserted chamber, and the bottom chamber was filled with 500.0  $\mu\text{L}$  of complete DMEM. After 12 h of incubation, the medium was removed. The cells in the membrane were washed by PBS and fixed using 4% (*W/V*) PBS-buffered paraformaldehyde. Finally, the cells were stained by crystal violet and then observed on a microscope (Nikon Eclipse *Ti*, Optical Apparatus Co., Ardmore, PA, USA).

***In Vivo* Targeting to Primary and Metastatic Tumors.** Green fluorescent protein-transfected B16F10 cells (B16F10-GFP) was prepared by lentivirus transduction in Figure S9. Human embryonal kidney (HEK) 293FT cells were firstly transfected with the plasmid mixture containing 10.0  $\mu\text{g}$  of EGFP transfer vector plasmid, 3.3  $\mu\text{g}$  of VSV-G plasmid, 6.67  $\mu\text{g}$  of pMDLg/pRRE plasmid, and 6.67  $\mu\text{g}$  of pRSV-Rev plasmid using Lipofectamine 2000 (Lipo2000) for 6 h. The cells were incubated with fresh medium for another 48 h. The supernatants were pooled together, passed through a 0.45  $\mu\text{m}$  filter, concentrated by ultracentrifugation at 50,000 g for 120 min, and stored at  $-80^\circ\text{C}$  until use. B16F10 cells were cultured until they reached 80% confluency in a 24-well culture plate. Then, 1.0 mL of Lentiviral vector solution containing 20.0  $\mu\text{L}$  of Lentiviral vectors was added into the well of B16F10 cells, and the cells were incubated at  $37^\circ\text{C}$  for 48 h. GFP-positive cells were purified using a BD Influx cell sorter (BD Biosciences, San Jose, USA) with a purity of 100%. The collected B16F10-GFP cells were cultured for two weeks, and the purity of GFP-positive cells were analyzed by FCM to make sure the purity was more than 99%.

C57/BL mice bearing primary B16F10-GFP tumor were obtained by injecting subcutaneously with B16F10-GFP cells ( $1 \times 10^7$  cells  $\text{mL}^{-1}$ , 100  $\mu\text{L}$  per mouse). When the tumor grown to about 200  $\text{mm}^3$ , the mice were treated with PBS, DOX, PNG/DOX, or PMNG/DOX at an equivalent DOX dose of 5.0 mg per kg body weight ( $\text{mg (kg BW)}^{-1}$ ). After 12 h of treatment, the mice were sacrificed and the tumors were collected. Subsequently, about 1 g of tumors were homogenized and resuspended in 10.0 mL of PBS. The samples were analyzed by FCM. Data for 10,000 gated events were collected.

C57/BL mice bearing metastatic melanoma were constructed by intravenously injection of B16F10 cells ( $1 \times 10^7$  cells  $\text{mL}^{-1}$ , 100  $\mu\text{L}$  per mouse). After 15 days, the mice were treated with PBS, DOX, PNG/DOX, or PMNG/DOX at an equivalent DOX dose of 5.0 mg ( $\text{kg BW}^{-1}$ ). After 12 h of treatment, the mice were sacrificed and the lungs were isolated. One piece of the lung was then homogenized and resuspended in 10.0 mL of PBS. Another piece of lungs was frozen and cut into 10  $\mu\text{m}$  slices. The lung sections were stained by 4',6-diamidino-2-phenylindole (DAPI) for 5 min and washed thrice by PBS. Afterwards, the slices were observed by CLSM.

**Plasma Clearance, Tumor Accumulation, and Biodistribution.** To analyze the fate of DOX-loaded nanogels *in vivo*, Sprague-Dawley rats were administrated with free DOX, PNG/DOX, or PMNG/DOX by tail vein injection. At predetermined time intervals (0.3, 0.5, 1, 2, 4, 8, 12, and 24 h), 500.0  $\mu\text{L}$  of blood was collected from the orbital venous plexus, heparinized, and centrifuged to obtain the plasma. Subsequently, 1.0 mL of acetonitrile was added into the plasma for protein settlement. After centrifugation at 12,000 rpm for 5 min, the supernatant was collected and dried under the nitrogen stream. Finally, the obtained residues



were redissolved in 300.0  $\mu\text{L}$  of acetonitrile for high-performance liquid chromatographic (HPLC) detection, which were performed on a Waters e2695 HPLC system equipped with Waters 2487 two-channel fluorescence detector and a Symmetry C18 column (Waters, Milford, MA, USA). Acetonitrile–water (30:70,  $V/V$ , pH 3.5) was used as an elution at a flow rate of 1.0  $\text{mL min}^{-1}$ . Fluorescence detector was set at 480 nm for excitation and 590 nm for emission, and linked to Breeze software for data analyses.

The tumor accumulation and biodistribution were examined as follow. C57/BL mice were injected subcutaneously and intravenously with B16F10 cells ( $1 \times 10^7$  cells  $\text{mL}^{-1}$ , 100  $\mu\text{L}$  per mouse). When the tumor volumes grew to about 200  $\text{mm}^3$ , free DOX, PNG/DOX, or PMNG/DOX was intravenously injected by the tail vein at an equivalent DOX dose of 5.0  $\text{mg (kg BW)}^{-1}$ . Mice were then sacrificed after 12 h. Tumor samples were homogenized in the solution with 5.0 mL of methanol and 5.0 mL of distilled water. Then, the homogenized samples were centrifuged at 3000 rpm for 10 min. The supernatants were collected, dried, and redissolved in the same way as introduced above. The concentration of DOX was also measured by HPLC as described before. The heart, liver, spleen, lung, and kidney were collected and imaged using the Maestro *in vivo* fluorescent imaging system (Cambridge Research & Instrumentation Inc., Woburn, USA). In addition, the average signals were also semiquantitatively analyzed using ImageJ software (National Institutes of Health, Bethesda, USA).

***In Vivo* Antitumor Efficacy against Primary Tumor.** C57/BL mice were injected subcutaneously with B16F10 cells ( $1 \times 10^7$  cells  $\text{mL}^{-1}$ , 100  $\mu\text{L}$  per mouse) and were allowed to grow to about 50  $\text{mm}^3$ . Then, the mice were randomly assigned to four groups ( $n = 8$ ). The

antitumor efficacies against primary tumors were evaluated by intravenously tail vein injection of PBS, DOX, PNG/DOX, or PMNG/DOX at an equivalent DOX dose of 5.0 mg (kg BW)<sup>-1</sup> for four times at a three-day interval. The antitumor efficacy was evaluated in terms of tumor volumes estimated by the following Equation 3:

$$V = \frac{a \times b^2}{2} \quad (3)$$

In Equation 3, *a* and *b* were the major and minor axes of the tumor measured by a caliper, respectively.

***In Vivo* Antitumor Efficiency against Lung Metastasis.** Mice with lung metastases were obtained by intravenously injection of B16F10 cells ( $1 \times 10^7$  cells mL<sup>-1</sup>, 100 µL per mouse). Then the mice were randomly assigned into four groups (*n* = 15), and the antitumor efficacies against metastatic tumors were evaluated by intravenously injection of PBS, DOX, PNG/DOX, or PMNG/DOX at an equivalent DOX dose of 5.0 mg (kg BW)<sup>-1</sup> for four times at a three-day interval. At the 15<sup>th</sup> day of the experiments, three mice in each group were sacrificed, and the lungs were stripped for further evaluation of the antitumor efficacies against lung metastasis. The survival rates were calculated by the other mice till 30<sup>th</sup> day of the experiment.

**Histological and Immunohistochemical Staining.** The tumors and lungs were collected, fixed in 4% (*W/V*) PBS-buffered paraformaldehyde overnight, and then embedded in paraffin. The paraffin-embedded tissues were then cut into about 5.0 µm slices for hematoxylin and eosin (H&E) staining and immunohistochemical analyses. The H&E staining were detected by a microscope (Nikon Eclipse *Ti*, Optical Apparatus Co., Ardmore, PA, USA) and subsequently analyzed with ImageJ software.

***In Situ* TUNEL Assays.** The paraffin-embedded tumors were cut into slices at a thickness of about 5  $\mu\text{m}$ , and then a terminal deoxynucleotidyl transferase-mediated deoxyuridine triphosphate nick-end labeling (TUNEL) assay was performed with a commercial kit following the manufacturer's instruction. The fluorescence microimages of tumor tissue sections were obtained through a CLSM.

**Statistical Analyses.** All experiments were performed at least three times, and the data were presented as mean  $\pm$  standard deviation (SD). Differences between experimental groups were assessed by *t*-test or log-rank test with statistical software SPSS 17.0 (SPSS Inc., Chicago, IL, USA).  $*P < 0.05$  was considered statistically significant, and  $**P < 0.01$  and  $***P < 0.001$  were considered highly significant.

## REFERENCES

1. Chen, C.; Wang, Z.; Li, Z. *Biomacromolecules* **2011**, 12, (8), 2859–2863.
2. Ding, J.; Shi, F.; Xiao, C.; Lin, L.; Chen, L.; He, C.; Zhuang, X.; Chen, X. *Polym. Chem.* **2011**, 2, (12), 2857–2864.
3. Albini, A.; Iwamoto, Y.; Kleinman, H. K.; Martin, G. R.; Aaronson, S. A.; Kozlowski, J. M.; McEwan, R. N. *Cancer Res.* **1987**, 47, (12), 3239–3245.

**Table S1.** Characterizations of PNG and PMNG. The results were evaluated by element analyses.

Entry	Unit Numbers of Moieties		
	$n(\text{mTEGLG})^{\text{a}}$	$n(\text{LP})^{\text{b}}$	$n(\text{LC})^{\text{c}}$
PNG	7.69	9.50	5.10
PMNG	7.59	8.95	6.50

<sup>a</sup>mTEGLG, <sup>b</sup>LP, and <sup>c</sup>LC were the abbreviations of  $\gamma$ -(methoxy tri(ethylene glycol))-L-glutamate, L-phenylalanine, and L-cystine, respectively.

**Table S2.** Quantitative pharmacokinetics data.

Entry	DOX	PNG/DOX	PMNG/DOX
$t_{1/2}$ (h)	8.2	13.0	28.1
$C_{\text{max}}$ ( $\mu\text{g mL}^{-1}$ )	16.0	34.9	51.9
$\text{AUC}_{\text{all}}$ ( $\mu\text{g mL}^{-1} \text{ h}$ )	110.5	329.7	386.9

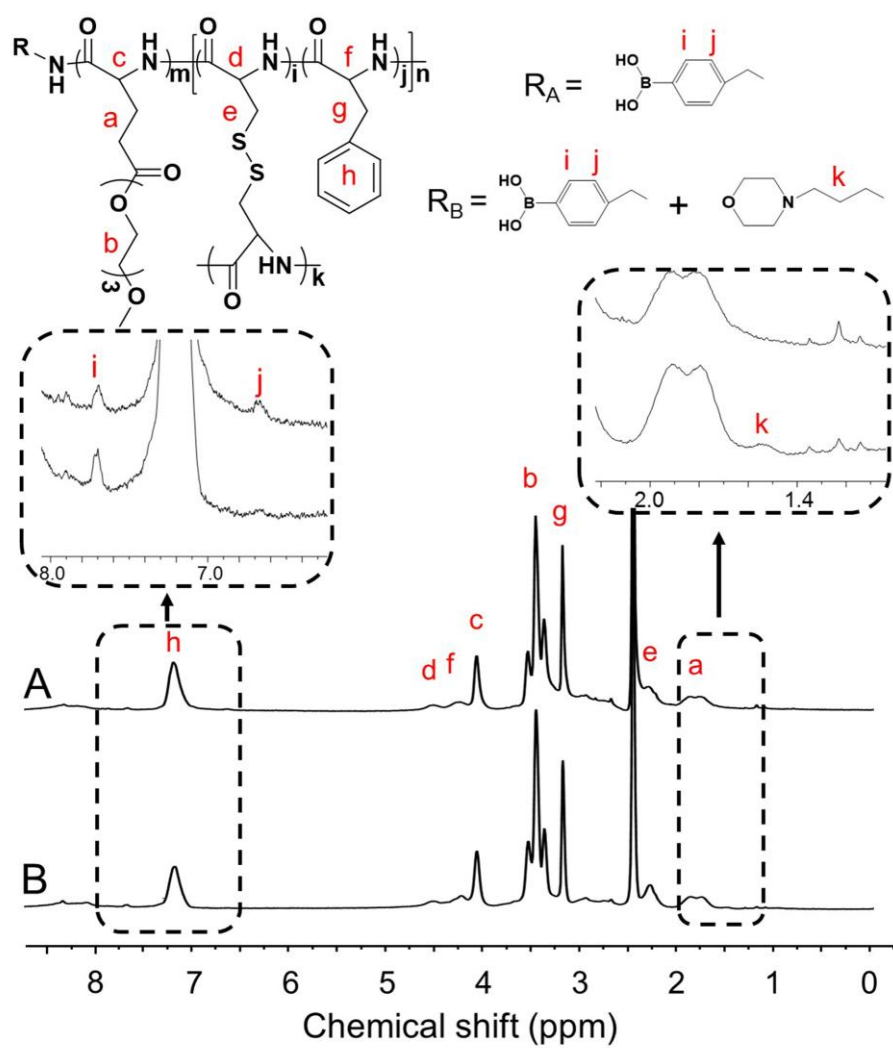


**Figure S1.**  $^1\text{H}$  NMR spectra of PNG (A) and PMNG (B) using dimethyl sulfoxide- $d_6$  (DMSO- $d_6$ ) as a solvent.

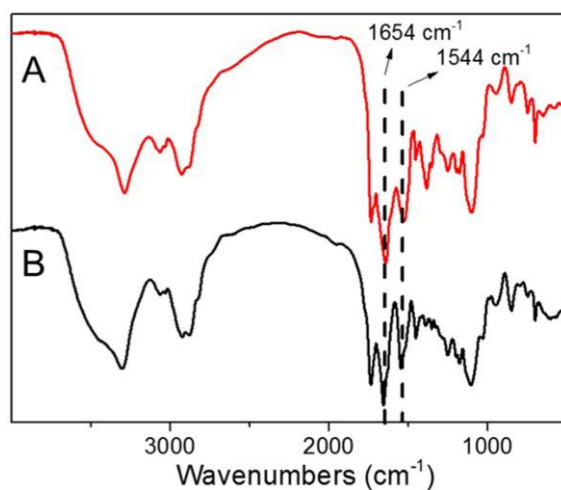


**Figure S2. FT IR spectra of PNG (A) and PMNG (B).** Typical absorptions of amide bond at 1654  $\text{cm}^{-1}$  ( $\nu_{\text{C=O}}$ ) and 1544  $\text{cm}^{-1}$  ( $\nu_{\text{C(O)-NH}}$ ) proved the successful polymerization of *N*-carboxyanhydrides.

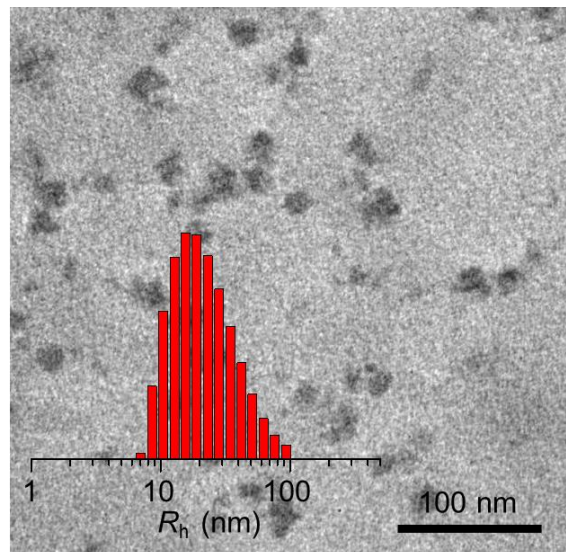


**Figure S3.** Typical TEM image and DLS (inset) of PNG.

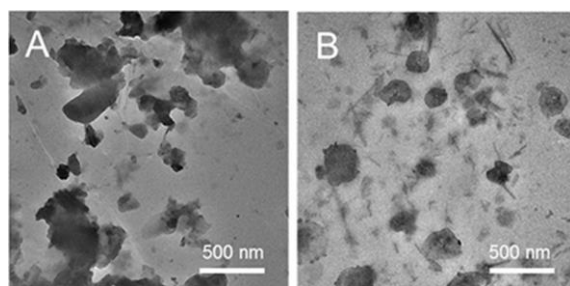


**Figure S4. Typical TEM images of PNG (A) and PMNG (B) incubated with GSH.** PNG and PMNG were incubated with 10.0 mM GSH, *i.e.*, simulation of intracellular reductive environment, for 8 h. As shown in the figure, the nanogels disassembled owing to the breakdown of the disulfide bond in the cores.



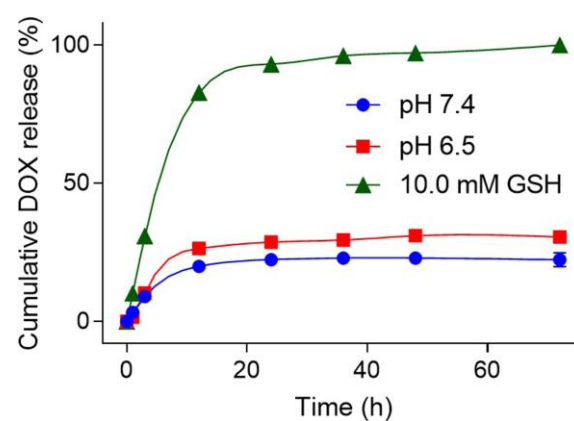


**Figure S5. DOX release behavior of PNG/DOX.** The DOX release behavior of PNG was carried out at pH 7.4, 6.5, and in the presence of 10 mM GSH. A GSH-accelerated DOX release was demonstrated due to the disassembly of disulfide bond-cross-linked core under reductive condition.

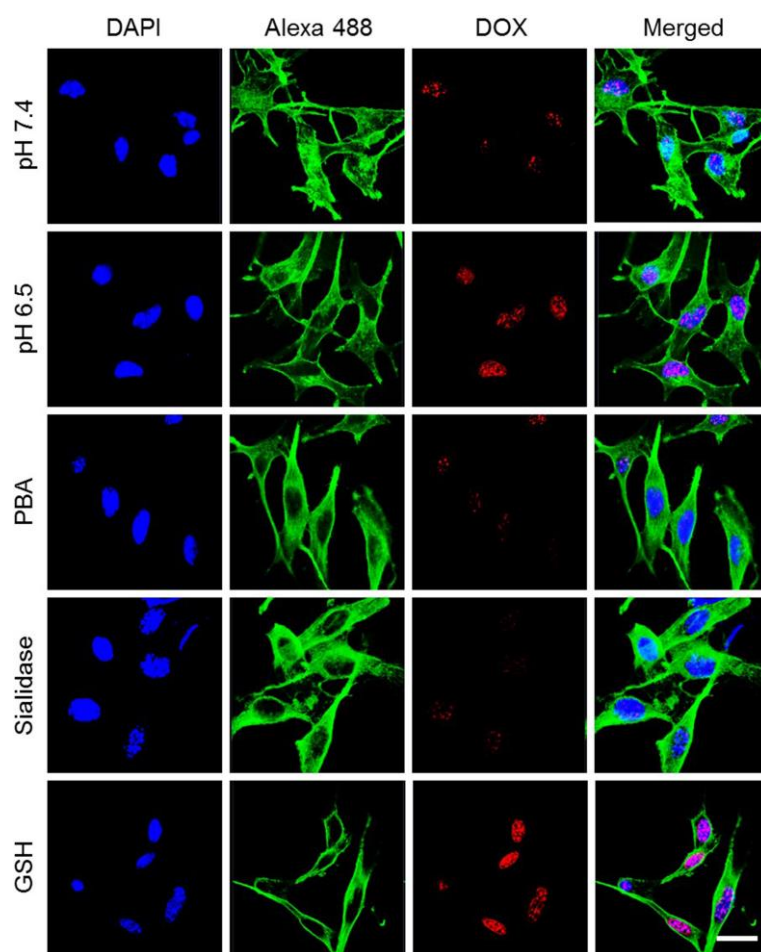


**Figure S6. CLSM images of B16F10 cells after incubation with PNG/DOX.** Cells were incubated in PBS at pH 7.4, 6.5, or 7.4 pretreated with 10.0 mM GSH for 3 h. To cleave SA specifically, the cells were pretreated with PBA (4.0 mM) or sialidase (40.0 mU ml<sup>-1</sup>) before the incubation with PNG. The cell nucleus was stained blue. The actin protein was stained green. The DOX fluorescence was marked as red. Scale bar = 50.0  $\mu$ m. The pretreatment of free PBA and sialidase significantly decreased cell uptake, which confirmed that the targeting efficiency of PNG was based on the interaction between the SA and PBA groups. Moreover, the GSH-enhanced DOX signal also indicated the reduction-accelerated DOX release under intracellular condition.

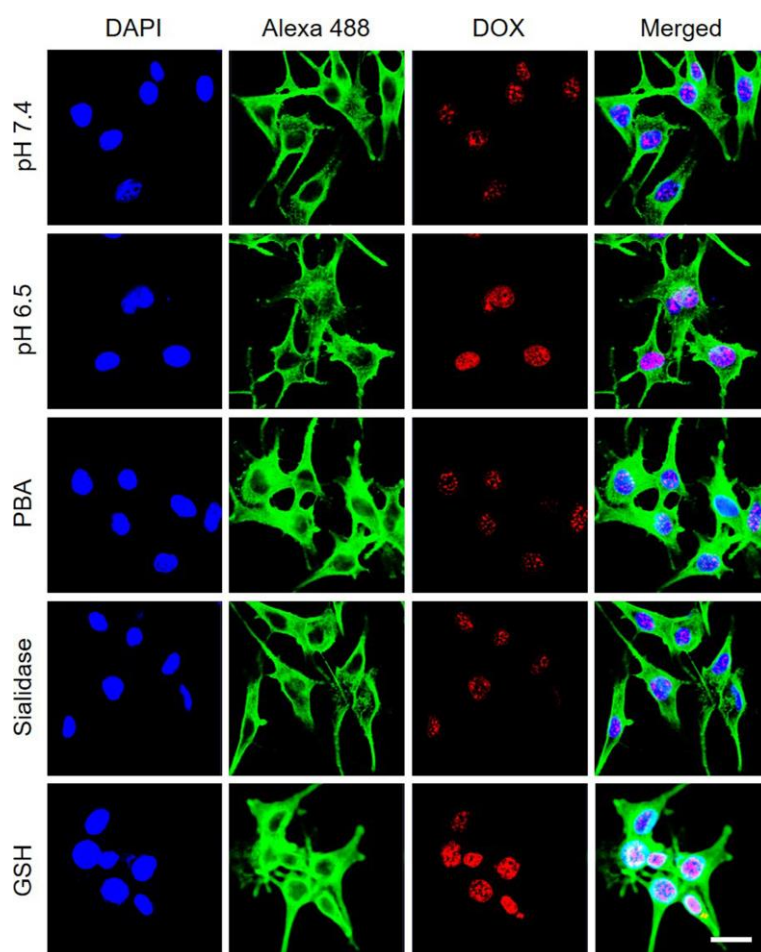


**Figure S7. CLSM images of B16F10 cells after incubation with PMNG/DOX.** Cells were incubated in PBS at pH 7.4, 6.5, or 7.4 pretreated with 10.0 mM GSH for 3 h. To cleave SA specifically, the cells were pretreated with PBA (4.0 mM) or sialidase (40.0 mU ml<sup>-1</sup>) before the coincubation with PMNG. The cell nucleus was stained blue. The actin protein was stained green. The DOX fluorescence was marked as red. Scale bar = 50  $\mu$ m. The pretreatment of free PBA and sialidase slightly decreased cell uptake compared to that of PNG in Figure S6, which indicated that the promoted targeting efficiency of PMNG was not only based on the interaction between the SA and PBA groups, but also the negatively charged cell membrane and the positively charged MP group. Also, the GSH-enhanced DOX signal also confirmed the reduction-accelerated DOX release under intracellular condition.

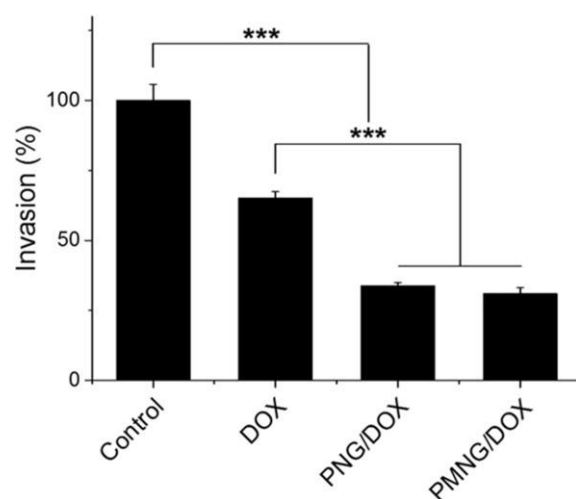


**Figure S8. Relative invasion abilities of B16F10 cells.** The B16F10 cells were treated with free DOX, PNG/DOX, or PMMG/DOX at an equivalent DOX concentration of  $1.0 \mu\text{g mL}^{-1}$ . Data were represented as mean  $\pm$  SD ( $n = 3$ ,  $t$ -test;  $*P < 0.05$ ,  $**P < 0.01$ ,  $***P < 0.001$ ). PNG/DOX and PMNG/DOX significantly decreased the cell invasion compared with free DOX.

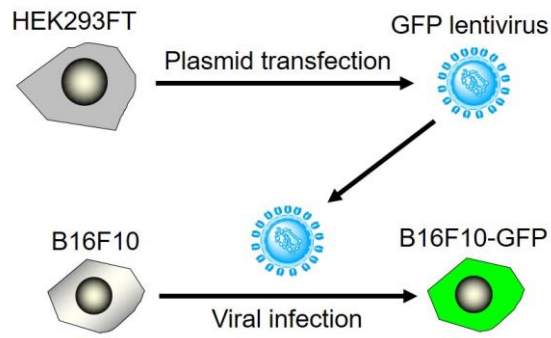


**Figure S9. Schematic illustration of B16F10-GFP cell preparation.** The GFP lentivirus was produced in HEK293FT cells by plasmid transfection. The B16F10 cells were infected by the lentivirus to produce GFP stably expressing cells.

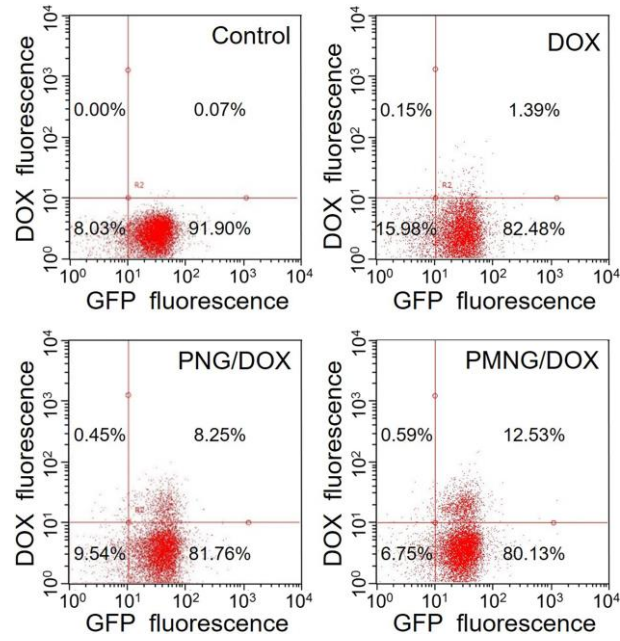


**Figure S10. Flow cytometry analyses of primary tumor cells.** The mice were treated with different formulations at an equivalent DOX concentration of  $5.0 \text{ mg (kg BW)}^{-1}$  for 12 h.

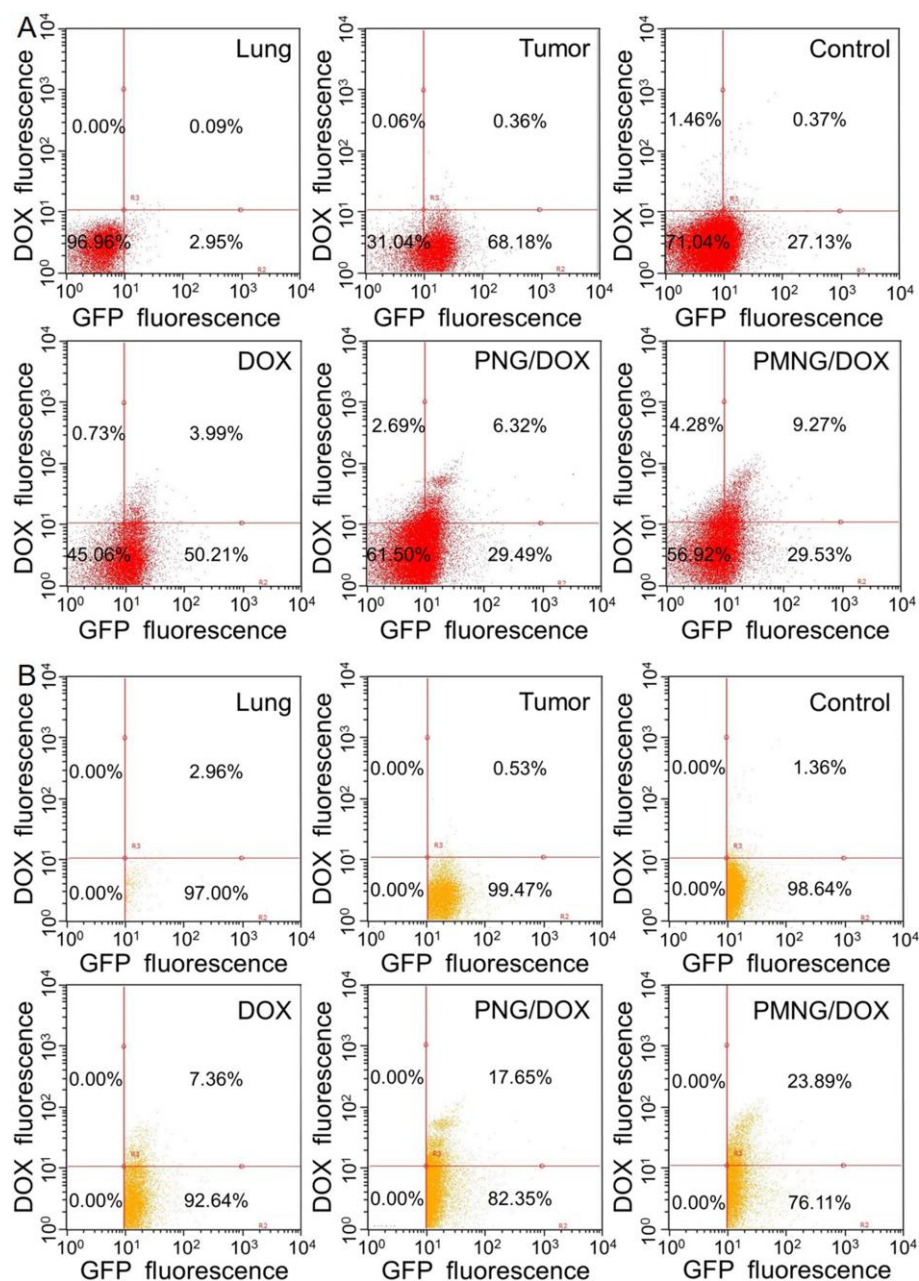


**Figure S11. Flow cytometry analyses of metastatic tumor cells.** (A) Flow cytometry analyses of cells collected from metastatic lungs after the treatment with different formulations at an equivalent DOX concentration of  $5.0 \text{ mg (kg BW)}^{-1}$  for 12 h. (B) Flow cytometry analysis of GFP-positive metastatic tumor cells. The blank lung and tumor were used to confirm the test condition.

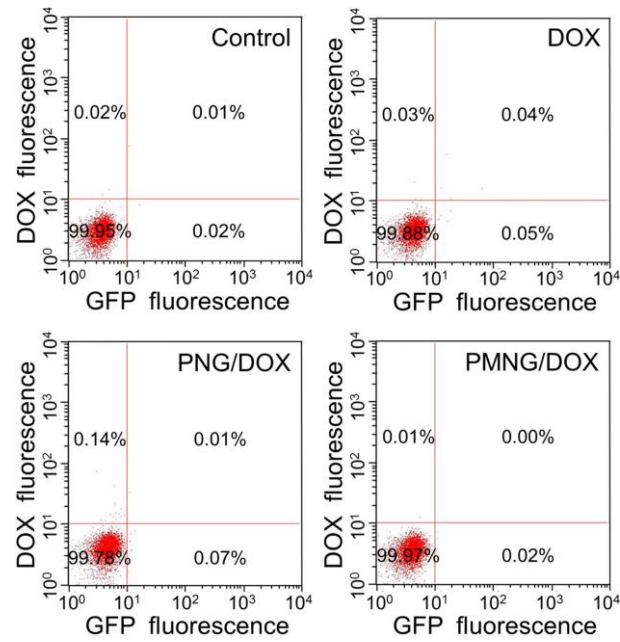


**Figure S12. Flow cytometry analyses of red blood cells.** The mice were treated with different formulations at an equivalent DOX concentration of  $5.0 \text{ mg (kg BW)}^{-1}$  for 12 h.



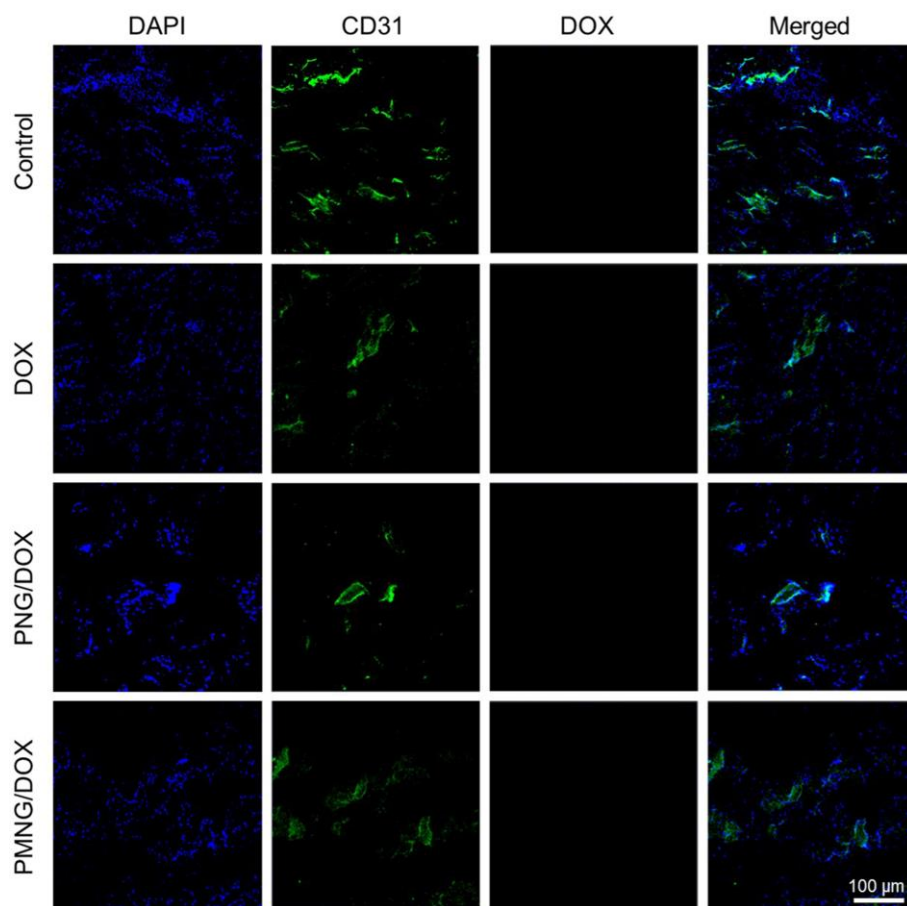


**Figure S13. CLSM images of normal tissue.** The mice were treated with different formulations at an equivalent DOX concentration of  $5.0 \text{ mg (kg BW)}^{-1}$  for 12 h. The nucleus was stained by DAPI. The blood vessels were stained by anti-CD31 antibody and then marked with FITC-conjugated secondary antibody.

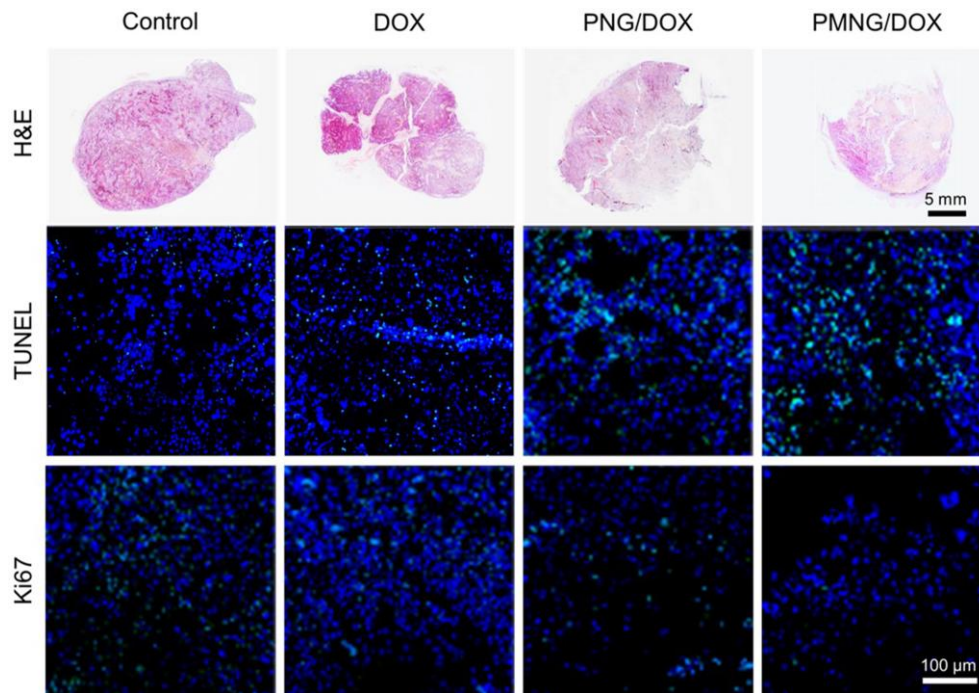


**Figure S14. H&E, TUNEL, and Ki67 staining of primary tumor.** At the end of primary tumor inhibition, the primary tumors were collected and cut into 5 μm slices. In H&E staining, cell nucleus was stained blue, and extracellular matrix and cytoplasm were stained red. In TUNEL assay, the broken DNA was stained with FITC-labeled deoxyuridine triphosphate (green). In Ki67 staining, the Ki67 proliferation antigen was stained with FITC-labeled secondary antibody (green).

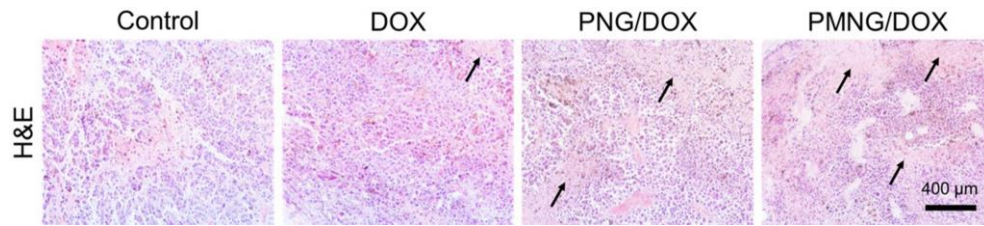


**Figure S15. Typical H&E images of primary tumor.** The apoptosis area was marked by black arrow. The black arrows pointed out the apoptosis regions.

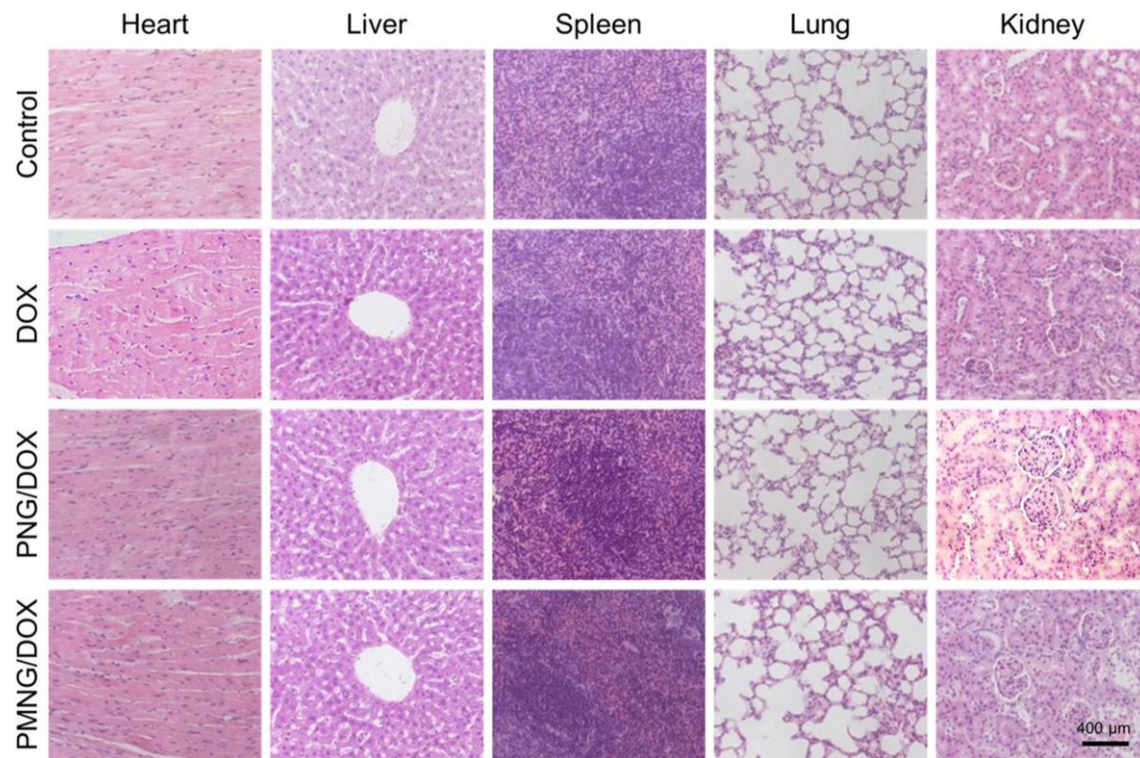


**Figure S16. Typical H&E images of major organs.** The major organs, *e.g.*, the heart, liver, spleen, lung, and kidney, were collected and cut into 5  $\mu\text{m}$  slices at the end of primary tumor inhibition.

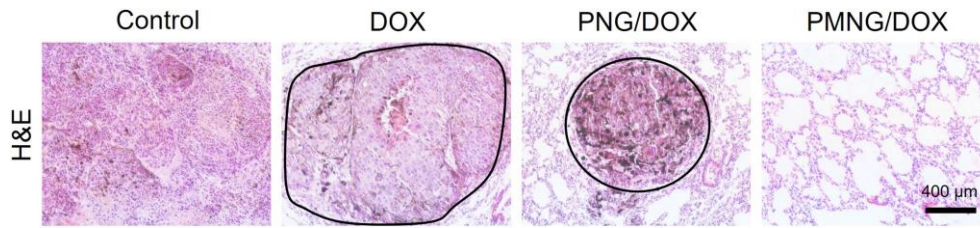


**Figure S17. Typical H&E images of lung metastasis.** The lungs were collected and cut into 5  $\mu\text{m}$  slices at the end of metastatic tumor inhibition. The metastatic foci were marked with black circle. In the control group, the whole picture was filled with metastatic foci. The significantly decreased metastatic foci in the PMNG/DOX group further confirmed its desirable anti-metastatic efficacy.